Published in final edited form as:
Neuroscience. 2010 August 25; 169(2): 920–931. doi:10.1016/j.neuroscience.2010.05.026.

The expression of Twisted gastrulation in postnatal mouse brain and functional implications

Mu Sun[1,2], **Cynthia Forsman**[1,3], **Consolato Sergi**[4,5], **Rajaram Gopalakrishnan**[6], **Michael B. O'Connor**[1,2], and **Anna Petryk**[1,3,*]

[1] Department of Genetics, Cell Biology and Development, University of Minnesota, Minneapolis, MN 55455-0356, USA

[2] Howard Hughes Medical Institute, University of Minnesota, Minneapolis, MN 55455-0356, USA

[3] Department of Pediatrics, University of Minnesota, Minneapolis, MN 55455-0356, USA

[4] Department of Laboratory Medicine & Pathology, University of Alberta, Alberta, Canada T6G 2B7

[5] Institute of Pathology, Medical University of Innsbruck, Innsbruck, Austria

[6] Diagnostic/Biological Sciences, School of Dentistry, University of Minnesota, Minneapolis, MN 55455-0356, USA

Abstract

Twisted gastrulation (TWSG1), an extracellular regulator of bone morphogenetic protein (BMP) signaling, is critical for embryonic brain development. Mice deficient in TWSG1 have abnormal forebrain development manifesting as holoprosencephaly. The expression and potential roles of TWSG1 in postnatal brain development are less well understood. We show that *Twsg1* is expressed in the adult mouse brain in the choroid plexus (CP), hippocampus, and other regions, with the strongest expression observed in CP. TWSG1 was also detected in a human fetal brain at mid-gestation, with highest levels in the epithelium of CP. *Bmp1, Bmp2, Bmp4-Bmp7* as well as *BmprIA* and *BmprII*, but not *BmprIB*, were expressed in CP. BMP antagonists *Chordin (Chrd)* and *Noggin* were not detected in CP, however *Chrd-like 1* and *brain-specific Chrd-like (Brorin)* were expressed. Electrophysiological study of synaptic plasticity revealed normal paired-pulse facilitation and long-term potentiation in the CA1 region of hippocampus in *Twsg1*$^{-/-}$ mice. Among the homozygous mutants that survive beyond the first 2 weeks, the prevalence of hydrocephalus is 4.3%, compared to 1.5% in a wild type colony (p=0.0133) between 3 and 10 weeks of life. We detected a high level of BMP signaling in CP in wild type adult mice that was 17-fold higher than in the hippocampus (p=0.005). In contrast, TGFβ signaling was predominant in the hippocampus. Both BMP signaling and the expression of BMP downstream targets *Msx1* and *Msx2* were reduced in CP in *Twsg1*$^{-/-}$ mice. In summary, we show that *Twsg1* is expressed in the adult mouse and human fetal CP. We also show that BMP is a branch of TGFβ superfamily that is dominant in CP. This presents an interesting avenue for future research in light of the novel roles of CP in neural progenitor differentiation and neuronal repair, especially since TWSG1 appears to be the main regulator of BMP present in CP.

Keywords

Twsg1; chordin-like; hydrocephalus; cerebrospinal fluid; choroid plexus; BMP

[*]To whom correspondence should be addressed: Anna Petryk, M.D., University of Minnesota, 13-124 PWB, MMC 8404, 516 Delaware Street, SE, Minneapolis, MN 55455, Phone: 612-624-5409, Fax: 612-626-5262, petry005@umn.edu.

Bone morphogenetic proteins (BMPs), members of the transforming growth factor beta (TGFβ) superfamily, are critical for prenatal development of the nervous system. BMPs regulate numerous processes, including neural induction, neural crest formation, axon guidance, spinal cord patterning, neuronal lineage commitment, and differentiation (Mehler et al., 1997, Liu and Niswander, 2005). The activity of BMPs is modulated in the extracellular space by several BMP-binding proteins, such as Follistatin, Noggin (NOG), Chordin (CHRD), Twisted gastrulation (TWSG1) and others (Balemans and Van Hul, 2002), which regulate binding of BMPs to their receptors and subsequent activation of both Smad-dependent and Smad-independent pathways (Sieber et al., 2009). In fact, it is the antagonism of BMP signaling that is necessary for neural induction and neurulation (Delaune et al., 2005, Di-Gregorio et al., 2007, Ybot-Gonzalez et al., 2007). Mice that are deficient in BMP antagonists NOG and CHRD (Anderson et al., 2002) or TWSG1 (Petryk et al., 2004) have severe defects in forebrain, midface, and jaw development, designated as otocephaly, a phenotype that resembles agnathia-holoprosencephaly complex in humans (Schiffer et al., 2002).

While the roles of BMPs during embryonic development have been extensively studied in vertebrates, their roles in postnatal brain function are less well understood. BMPs and their receptors are expressed in several regions in the adult rodent brain, including the hippocampus and the choroid plexus, suggesting their continued physiological function (Soderstrom et al., 1996, Ebendal et al., 1998, Soderstrom and Ebendal, 1999, Scott et al., 2000, Fan et al., 2003). In the hippocampus, BMPs as well as NOG and CHRD regulate neurogenesis (Tang et al., 2009), synaptic plasticity and learning behavior through a presynaptic mechanism (Sun et al., 2007). Recent evidence suggests that inhibition of BMP signaling by NOG promotes expansion of neural stem cells isolated from the adult hippocampus (Bonaguidi et al., 2008). Several growth factors, including BMP7 and TGFβ1, are expressed in the choroid plexus and are present at high concentrations in adult cerebrospinal fluid (CSF) (Johanson et al., 2000, Dattatreyamurty et al., 2001). BMP7 that is contained in the CSF can induce dendritic growth in rat synaptic neurons. This activity is inhibited by Follistatin, which is a BMP antagonist (Dattatreyamurty et al., 2001). Thus, it seems that there are numerous emerging roles for the BMPs in the adult brain.

Regulation of BMPs by BMP-binding proteins plays a central role in controlling ligand availability and threshold dependent biological outcomes. While there is some evidence for the roles of NOG, CHRD, and Follistatin in BMP function in adult rodent brain, much less is known about the postnatal expression and function of TWSG1. TWSG1 can bind and inhibit BMP activity either directly or in a complex with CHRD (Ross et al., 2001, Petryk et al., 2005, Wills et al., 2006). TWSG1 may also enhance BMP signaling by promoting degradation of CHRD by Tolloid and CHRD-independent mechanisms (Larrain et al., 2001, Zakin and De Robertis, 2004). We have previously reported 44% incidence of HPE in *Twsg1* homozygous mutant mice in C57BL/6 background that, along with craniofacial defects, leads to neonatal lethality (Petryk et al., 2004, MacKenzie et al., 2009). The purpose of this paper was to examine whether *Twsg1* is expressed in the adult mouse brain in the areas in which *Bmps* and their receptors are expressed, identify the molecules with which TWSG1 could potentially interact in these regions to modulate BMP signaling, and determine whether those mutants that do not manifest overt HPE and survive beyond the neonatal period have any evidence of neurologic impairment.

EXPERIMENTAL PROCEDURES

Animals

Generation and genotyping of *Twsg1*$^{-/-}$ mice in C57BL/6 background were performed as previously described (Petryk et al., 2004). Wild type (WT) C57BL/6 mice were obtained from Taconic Farms, Inc. (Albany, NY, USA). Age-matched *Twsg1*$^{-/-}$ and control male mice at 1–3 months of age were used in this study following protocols approved by the University of Minnesota Institutional Animal Care and Use Committee.

RT- PCR and Real-time Q-PCR

Total RNA was extracted from tissues with TRIzol Reagent (Invitrogen, Carlsbad, CA, USA) and purified using RNeasy (Qiagen, Valencia, CA, USA). Each RNA column was treated with DNase I to remove genomic DNA. First strand cDNA was synthesized from total RNA (3μg) using SuperScript III System (Invitrogen) with oligo(dT)20 primer in a total reaction mixture of 20 μl. Each reaction was diluted with distilled water to a final volume of 50 μl and 1 μl of the cDNA pool was subject to RT-PCR or Q-PCR analysis with primer pairs designed by PerlPrimer (Marshall, 2004). Primer sequences are included in Table 1. Primers for *Msx1* (Park et al., 2006) and *Msx2* (Berdal et al., 2009) were previously published. RT-PCR conditions were 94°C for 6 min: 1cycle, followed by 94°C for 45 sec, 58°C for 45 sec, and 72°C for 45 sec: 30 cycles and 72°C for 10 minutes.

Q-PCR was carried out by Roche LC480 system using SYBR Green PCR Master I (Roche) in a final volume of 20 μl. PCR conditions were 95°C for 5min: 1cycle, followed by 95°C for 10 sec, 58°C for 10 sec, and 72°C for 20 sec: 45 cycles. The transcriptional levels were normalized with *β-actin* transcriptional levels in the same samples. The expression level of *Twsg1* in CP was calibrated as 1. Triplicate measures of each sample were conducted to ensure the consistency of the amplification. Data were analyzed with Roche LightCycler 480 SW1.5.

Western blot

Mouse brain tissue was harvested from adult C57BL/6 mice, homogenized, passed through a 20G needle in modified RIPA buffer (50 mM Tris-HCl pH 7.4, 150 mM NaCl, 1% Triton x-100, 1% sodium deoxycholate, 0.1% SDS, 1 mM EDTA) and centrifuged for 10min at 4 °C. Brain homogenates were separated by SDS-PAGE followed by transfer onto PVDF membranes and blocked with Odyssey blocking buffer (LI-COR, Lincoln, NE) containing 0.1% (v/v) Tween 20. Membranes were incubated overnight at 4° C with anti-P-Smad1/5/8 (Cell Signaling Technology, Danvers, MA) (1:250), anti-P-Smad2 (Cell Signaling Technology) (1:1000), and anti-GAPDH (ABCam, Cambridge, MA) (1:5000) antibodies and washed before incubation with species-appropriate fluorescent conjugated secondary antibodies for 1h at room temperature. After washing to remove trace detergent, membranes were analyzed using an Odyssey Infrared Imaging System (LI-COR; Millennium Science, Surrey Hills, Australia) using the manufacturer's protocol.

Immunostaining of mouse brains

Brains were perfused with 10% buffered formalin and embedded in 2% agarose, 50 μm coronal sections were cut with vibrating-blade microtome (Leica VT1000s, Nussloch, Germany) in cold PBS. Structure of brain ventricular systems was observed with DAPI staining under Zeiss LSM710 confocal microscope. Sections from adult mice were incubated with primary monoclonal anti-TWSG1 antibody at 1:100 (R&D), 4°C overnight. After incubation with fluorescently labeled secondary antibody (Alexa Fluor 555) at 1:200 for 1 hour at room temperature, Z stack images were captured and processed using a Zeiss

LSM710 confocal microscope. Sections without incubation of primary antibody served as control.

Extracellular field excitatory postsynaptic potential (EPSP) recordings, paired-pulse facilitation (PPF), and long-term potentiation (LTP)

Mice were decapitated after anesthesia, hippocampal slices (350 μm thick) were cut in ice-cold artificial CSF containing (in mM) 250 sucrose, 25 $NaHCO_3$, 25 glucose, 2.5 KCl, 1.25 NaH_2PO_4, 2 $CaCl_2$, and 1.5 $MgCl_2$ (pH 7.3, 320 mOsm). The slices were recovered in a submerged chamber at room temperature (24–25°C) in carbogen-bubbled ACSF, containing 125 mM NaCl in place of 250 mM sucrose, for at least 2 hours before the start of recordings. Recordings were made in a standard interface chamber at 30°C (Fine Science Tools, Foster City, CA, USA) with 1 ml/min perfusion speed. A test pulse is given by a custom designed platinum bipolar electrode (MX21CEPMS1, FHC) for stimulating Schaffer collaterals at 0.05 ms duration and every 20 seconds. Field excitatory postsynaptic potential (fEPSP) was recorded by 1–2MΩ glass recording in the stratum radiatum of CA1 in the hippocampal slice. Data were acquired through Axonclamp B and Pclamp 8 software. PPF was examined at 25, 50, 100, and 200 ms inter-stimulus intervals with stimulation strength correlated to 30% of the maximal fEPSP. Stimuli intensity correlated to 50% maximal fEPSP slope was used for baseline and induction of LTP. Induction protocol is theta burst stimulation (TBS) which entailed 4 trains of 10 bursts of 4 stimuli with 20 s, 200 ms, and 10 ms intervals between trains, burst, and stimuli, respectively (Sun et al., 2007).

Autopsy study

A legal autopsy was performed at the Institute of Pathology, Medical University of Innsbruck, Austria, following death of a human fetus for acute placental reasons at 23+ weeks gestation. The study was approved by the Institutional Ethics Committee. The measurements and body weight of the fetus were: 590 g, crown-heel length 30.5 cm, crown-rump length 21 cm, foot length 4.5 cm, occipitofrontal circumference 20.5 cm, biparietal diameter 5.8 cm, shoulder circumference 21.5 cm, thorax circumference 17 cm, abdominal circumference 19 cm, and pelvic circumference 14 cm. All values correspond to a fetus of 23 – 24 weeks of gestation. Examination of the central nervous system was performed by a pediatric pathologist (CS).

Immunohistochemistry

Immunohistochemistry was performed to examine localization of TWSG1 in the normal human fetal brain at mid-gestation. The specimens were fixed in 10% neutral buffered formalin for approximately 24 h at room temperature, cut into slices of 5 mm of thickness, embedded in paraffin blocks and sectioned serially at 5 μm thickness. After treatment with 0.5% H_2O_2 in methanol and blocking serum, these sections were incubated with monoclonal antibody against human TWSG1 (Novus Biologicals, Littleton, CO, USA) at 1:25 dilution at room temperature for 32 min. Subsequently, sections were incubated with Discovery Universal Secondary Antibody (Ventana Medical Systems, Tucson, AZ, USA), and automatically stained using a Ventana Autostainer (Discovery XT) with an avidin–biotin peroxidase complex method and counterstained with hematoxylin. Negative controls contained no primary antibody.

Statistics and data analysis

Unpaired *t* tests were used for mutants and control littermates for *in vitro* or *in vivo* experiments, with a Type I error rate of $\alpha = 0.05$ (two-tailed). All experimental data are expressed as mean ± SEM. A Chi-square test was performed to determine if the difference

in the incidence of hydrocephalus between WT and *Twsg1*$^{-/-}$ mice was statistically significant.

RESULTS

Expression pattern of *Twsg1* in a mouse adult brain

It has been previously shown that *Twsg1* is expressed in the developing mouse brain (particularly telencephalon) as early as the neural plate stage (Graf et al., 2001, Zakin et al., 2005). According to the Allen Mouse Brain Atlas (Allen Institute for Brain Science, Seattle, WA, USA), *Twsg1* is also expressed in the adult mouse brain in the choroid plexus, hippocampus, and cerebellum (Fig. 1A, B, also available from: http://mouse.brain-map.org) (Lein et al., 2007). Amplicons of *Twsg1* could be detected by RT-PCR in the hippocampus, choroid plexus, cerebellum and cortex isolated from 1-month-old WT mice, but not from *Twsg1*$^{-/-}$ mice (Fig. 1C). Q-PCR was performed to quantitate *Twsg1* expression in various brain regions (Fig. 1D). The highest level of expression was found in the choroid plexus, followed by cerebellum, thalamus, cortex, hippocampus, brain stem, and olfactory bulb. Presence of TWSG1 protein was confirmed by immunohistochemistry in the choroid plexus (Fig. 2A, C), hippocampus (Fig. 2E), specifically CA3 (Fig. 2F), cerebellum (Fig. 2G), and cortex (Fig 2H). TWSG1 was immunodetected on cell surface and in the extracellular matrix, consistent with it being a secreted protein (Melnick et al., 2006).

Distribution of TWSG1 in human fetal brain

To determine if TWSG1 can also be detected in a human brain, we elected to study a fetal brain at mid-gestation (23 weeks gestation), partly due to limited availability of a normal human adult brain tissue and also because many of the brain regions in which *Twsg1* is expressed in an adult brain are already present *in utero*. The molecular layer of the cerebral cortex was immunoreactive for TWSG1 (Fig. 3A, arrowheads). Cortical neurons were immunoreactive on the surface and remarkably, there was intense staining in the perikarya of some neurons with rosette pattern formation (Fig. 3B, arrows). No significant immunoreactivity was observed in the striatum and in the subcortical white matter (not shown). Ventricular neuroepithelium of the 4th ventricle showed moderate immunoreactivity (Fig. 3D). The strongest expression was observed in the choroid plexus (Fig. 3F with inset). From rostral to caudal all papillary projections of the choroid plexus showed an intense signal of the lining epithelium, while no signal was seen in the fibrovascular core of the papillary projections. In the cerebellum (not shown), TWSG1 was detected in the molecular layer, but not in the external granular layer. Immunoreactivity was seen in the perikarya of Purkinje cells. Weak immunoreactivity was detected in the internal granular layer. Expression in the dentate nucleus was faint. In all experiments negative controls showed no immunoreactivity for TWSG1.

Normal hippocampal synaptic function in *Twsg1*$^{-/-}$ mutants

Previously, we demonstrated that loss of CHRD, another potent BMP inhibitor, leads to enhanced synaptic plasticity and spatial learning suggesting a role for BMP signaling in regulating hippocampal activity (Sun et al., 2007). As there was high expression level of *Twsg1* in the hippocampus, we sought to determine if *Twsg1* mutants show similar synaptic defects in the hippocampus. To avoid the effect of severe morphological change on the function of the hippocampus, we used adult *Twsg1*$^{-/-}$ mice with a normal-appearing brain on gross and microscopic examinations. We found no significant difference in hippocampal long-term synaptic plasticity between *Twsg1* knockout mice and control mice. *Twsg1*$^{-/-}$ mice showed both normal LTP and PPF in the CA1 region of hippocampus (Fig. 4). Using field potential recordings from the CA1 region of the hippocampus, we found that *Twsg1*$^{-/-}$ mice showed normal excitatory transmission in the hippocampus compared to controls (Fig.

4A). PPF, a form of short-term plasticity between Schaffer collaterals and CA1 dendrites, was not significantly different in extracellular field recordings from *Twsg1* mutant slices (Fig. 4B). With a series of inter-pulse intervals, from 25ms to 200ms, *Twsg1*$^{-/-}$ slices showed a normal PPF ratio. With an interface chamber, TBS protocol induced robust LTP in both genotypes (WT, 152.49± 5.49 vs. *Twsg1*$^{-/-}$, 152.30± 5.85, p=0.98 Fig. 4C).

Severe hydrocephalus in TWSG1-deficient mice

The strongest expression of *Twsg1* was in the choroid plexus in both mice and humans. Since the main function of the choroid plexus is the production of CSF, we wanted to determine if and at what frequency *Twsg1*$^{-/-}$ mice manifest hydrocephalus. We previously reported that only 18% of *Twsg1*$^{-/-}$ mice in C57BL/6 background survive beyond the perinatal period (Petryk et al., 2004). The current survival rate is higher at 44% (297 out of 675 homozygotes), likely due to selective breeding techniques, which included the use of surviving homozygous males as breeders (Table 2). The frequency of craniofacial defects has not changed (45%). The remaining 11% of mice die either at birth or within the first 48 hours to 2 weeks of life without any external defects, suggesting that other organ systems may be involved. Among the homozygous mutants that survive beyond the first 2 weeks, 4.3% develop severe hydrocephalus (compared to 1.5% prevalence in our WT colony, p=0.0133) between 3 and 10 weeks of life, which is accompanied by significant growth failure, gait imbalance, lethargy, and closed eyes. The hydrocephalic *Twsg1*$^{-/-}$ mice have dome-shaped heads and increased brain volume (Fig. 5).

The coronal sections of enlarged brains from *Twsg1*$^{-/-}$ mice showed dramatic enlargement of the ventricles and thinning of the cerebral cortex (Fig. 6B, D) in comparison to WT control sections (Fig. 6A, C). The hippocampus of the mutants was compressed and pushed toward the midline, and the periaqueductal gray matter was compressed and atrophic (Fig. 6D). With continuous sectioning, we could not detect a clear opening within the aqueduct in hydrocephalic mutants (Fig. 6F, H), whereas in WT mice we could see a stepwise increase of the aqueduct's diameter from the third ventricle to the fourth ventricle (Fig. 6E, G). We did not detect any tumor-like structure inside the aqueduct of mutants, which argued against obstructive hydrocephalus. The fourth ventricle of *Twsg1*$^{-/-}$ mice showed normal morphology (Fig. 6J) and there was no overgrowth of the choroid plexus in any of the ventricles (Fig. 6L) compared to WT (Fig. 6I, K).

Identification of BMP ligands, receptors, and binding proteins in the choroid plexus

Since TWSG1 can interact with BMPs, CHRD, and CHRD-like proteins, we examined the expression of BMP ligands, their receptors, and antagonists in the choroid plexus and other brain regions (Fig. 7). We were particularly interested in identifying potential TWSG1 partners in the choroid plexus where *Twsg1* expression was the highest. All *Bmp*s tested (*Bmp1*, *Bmp2*, *Bmp4-Bmp7*) as well as *BmprIA* and *BmprII*, but not *BmprIB*, were expressed in the choroid plexus. *Chrd*, *Chrd-like 2* and *Nog* were not detected in the choroid plexus, however *Chrd-like 1* and *brain-specific Chrd-like (Brorin)* were expressed in the choroid plexus (as well as other brain regions), albeit at low levels.

Dominant role of BMP branch of the TGFβ pathway in choroid plexus and its regulation by TWSG1

While Smads 1, 5, and 8 are main signal transducers for the BMPs, Smads 2 and 3 serve mainly as substrates for the TGFβ pathway (Massague et al., 2005). We detected a very high level of BMP signaling in the choroid plexus in WT adult mice that was 17-fold higher than in the hippocampus (p=0.005) (Fig. 8A, B). In contrast, TGFβ signaling was predominant in the hippocampus, at a 1.8-fold higher level than in the choroid plexus (p=0.03). BMP signaling was significantly reduced in the choroid plexus in *Twsg1* mutants to approximately

20% signal intensity of the WT (p=0.042) (Fig. 8C, D), suggesting that TWSG1 acts as a BMP agonist in the choroid plexus. The level of P-Smad1,5,8 was very low in the hippocampus and there was no significant difference between WT and *Twsg1*$^{-/-}$ mice (not shown). The expression of downstream targets of BMP signaling, *Msx1* and *Msx2* (Ovchinnikov et al., 2006), was also reduced in the choroid plexus and the hippocampus in *Twsg1*$^{-/-}$ mice ($p<0.05$) (Fig. 9A, B).

DISCUSSION

The analysis of postnatal phenotype of *Twsg1*$^{-/-}$ mice in C57BL/6 background was previously hampered by high prevalence of perinatal lethality (Petryk et al., 2004). Increased survival of the mutants by using surviving homozygous males as breeders allowed us to study hippocampal function in these mice. We have previously shown that CHRD contributes to hippocampal plasticity and spatial learning and that *Chrd* null mice have increased presynaptic transmitter release from hippocampal neurons, resulting in enhanced PPF and LTP (Sun et al., 2007). Since TWSG1 and CHRD form tripartite complexes with BMPs, inhibiting their activity (Ross et al., 2001), and both are expressed in the hippocampus, we sought to determine if *Twsg1* mutants would show similar synaptic defects in the hippocampus. We found no significant difference in either PPF or LTP between *Twsg1*$^{-/-}$ and WT mice. This indicates that in spite of overlapping expression patterns, TWSG1 and CHRD may have different functions. Even though we did not find defects in synaptic plasticity in the absence of TWSG1, the function of BMPs in the hippocampus is not limited to regulating neuronal plasticity. Neurogenesis continues in adult life and inhibition of BMP signaling, for example by NOG, promotes the expansion of the hippocampal neural precursors *in vitro* (Bonaguidi et al., 2008).

The high level of expression of *Twsg1* and robust BMP signaling in the choroid plexus are intriguing. Choroid plexus is the main site of CSF secretion, although 10–30% of CSF also arises from the interstitial space (Brodbelt and Stoodley, 2007). CSF overproduction has been reported in mice (Lindeman et al., 1998), but it is a very rare cause of hydrocephalus in the absence of choroid plexus adenoma or carcinoma (Rickert and Paulus, 2001). Excessive production of CSF or insufficient reabsorption results in communicating hydrocephalus as opposed to non-communicating hydrocephalus due to CSF pathway obstruction (Zhang et al., 2006a). Hydrocephalus can also be divided into congenital and acquired. The latter is usually due to malformations, tumors, infections or hemorrhage that impair flow of the CSF. The most common cause of congenital hydrocephalus is stenosis of the aqueduct of Sylvius, although in some cases stenosis may also be the result, not the cause, of congenital hydrocephalus due to an increase in intracranial pressure (Landrieu et al., 1979, Willems et al., 1987). *Twsg1*$^{-/-}$ mice manifest postnatal hydrocephalus, but at a low incidence of 4.3% compared to 1.5% in our WT colony of C57BL/6 mice. True incidence may be higher, but is difficult to determine due to high (56%) perinatal mortality rate. The early onset of presentation of hydrocephalus in *Twsg1*$^{-/-}$ mice and absence of an obstructive lesion implycongenital communicating hydrocephalus with secondary aqueductal stenosis.

The exact mechanism of congenital hydrocephalus is not always clear. In mice overexpressing *Tgfβ1,* the primary mechanism is deposition of extracellular matrix molecules laminin and fibronectin in perivascular astrocytes, which presumably results in altered production and/or reabsorption of CSF (Galbreath et al., 1995, Wyss-Coray et al., 1995, Crews et al., 2004). Other proposed mechanisms include cortical thinning due to reduced proliferation of neural progenitor cells with secondary expansion of the ventricles (Zhang et al., 2006b), impaired function of the ciliated ependymal cells lining the ventricles (Davy and Robinson, 2003), disruption of neural cell adhesion (Rosenthal et al., 1992), or altered neural cell fate in neuroepithelial cells (Chae et al., 2004). Low incidence of

hydrocephalus in *Twsg1*$^{-/-}$ mice precludes detailed mechanistic studies. Cell-specific deletion or overexpression of *Twsg1* owing to a conditional design, for example in *Wnt1* cell lineages (Dietrich et al., 2009), may provide a better model to study the mechanism of hydrocephalus in these mice in the future. Reduction in BMP signaling in *Twsg1*$^{-/-}$ mice strongly implicates the role of BMP pathway in the pathogenesis of hydrocephalus. This is consistent with the observation that disruption of *Msx1*, a downstream target of BMPs, also leads to hydrocephalus (Ramos et al., 2004).

It is interesting to speculate that abnormal development of telencephalon and congenital hydrocephalus may be linked. For example, *Otx2* mutants in C57BL/6 background have severe loss of rostral head structures, while heterozygous mice display a spectrum of otocephalic phenotypes, similar to those observed in *Twsg1*$^{-/-}$ mice (Matsuo et al., 1995). Interestingly, in CBA background, 13% of heterozygotes develop hydrocephalus between 4 weeks and 6 months of life (Makiyama et al., 1997). Likewise, 80% of *Cdo*$^{-/-}$ mice manifest HPE due to reduced Sonic hedgehog signaling in the ventral forebrain (similar to *Twsg1*$^{-/-}$ mice), but those that survive beyond the perinatal period without overt signs of HPE develop hydrocephalus (Zhang et al., 2006b). Existence of either HPE or hydrocephalus in the same mouse knockouts and variable severity of the craniofacial phenotypes depending on the gene dosage and genetic background, suggest that these phenotypic manifestations may represent a continuum and that in spite of successful survival residual cellular defects persist and may lead to a later manifestation as hydrocephalus.

Aside from regulation of CSF production, choroid plexus regulates other processes during both embryonic and postnatal brain development and function. Choroid plexus forms early in embryogenesis and is already well differentiated at E12.5 in mice. It is a source of nutrients, morphogens, growth factors, and humoral factors that are important for maintaining brain homeostasis, including neurohumoral and neuroimmune interactions (Strazielle and Ghersi-Egea, 2000, Redzic et al., 2005). Recent studies provide evidence for novel roles of choroid plexus and BMPs contained in the CSF in differentiation of neural progenitors (Lim et al., 2000, Krizhanovsky and Ben-Arie, 2006, Buddensiek et al., 2009) and neuronal repair after ischemic brain injury (Johanson et al., 2000, Martinez et al., 2001). The BMP-mediated inhibition of neurogenesis can be blocked by BMP inhibitors, underscoring the importance of BMP regulation in this process. Upregulation of several growth factors, including *Tgfβ1*, has been observed in choroid plexus following ischemic and traumatic brain injury, suggesting the roles of growth factors in mediating epithelial recovery and brain repair (Johanson et al., 2000). Growth factors that are synthesized and secreted by the epithelial cells of the choroid plexus into the CSF may also affect other brain regions, for example the hippocampus. A regulatory role of TWSG1 cannot be excluded in neuronal repair, especially in light of the data that TWSG1, along with CHRD-like 1, regulate BMP homeostasis in the proximal tubule under normal conditions and during regeneration following ischemic kidney injury (Larman et al., 2009). *Chrd-like 1* is also expressed in the choroid plexus, placing it in the region conducive to its interactions with TWSG1. The similarity between the regenerative processes in the epithelia of the renal tubules and choroid plexus is further enhanced by the observation that TGFβ1 is upregulated in the epithelium of the renal tubules as well as choroid plexus following ischemic injury (Johanson et al., 2000).

In summary, we show that *Twsg1* is expressed in the adult mouse and human fetal choroid plexus. We also show that BMP is a branch of TGFβ superfamily that is dominant in the choroid plexus. This presents an interesting avenue for future research in light of the novel roles of choroid plexus in neural progenitor differentiation and neuronal repair, especially since TWSG1 appears to be the main regulator of BMP present in the choroid plexus. Presence of hydrocephalus and HPE in TWSG1-deficient mice suggests that congenital

hydrocephalus may be a developmental anomaly and mutations in developmental pathways (or their regulatory proteins) may contribute to the pathogenesis of this disease. Understanding the roles of growth factors in brain homeostasis has therapeutic implications because, as secreted factors, they can be administered intrathecally. For example, intraventricular administration of hepatocyte growth factor in a mouse model of TGFβ1-induced hydrocephalus results in an improved CSF flow and a reduction of ventriculomegaly (Tada et al., 2006). Expression of TWSG1 protein in fetal brain suggests a potential role for TWSG1 in normal human brain development as well.

Acknowledgments

M.B.O. is an Investigator with the Howard Hughes Medical Institute. This work was partially supported by the NIH grant R01 DE016601 to A.P. The authors would like to thank Dr. Lothar Resch (University of Alberta Hospital) and Charles Billington (University of Minnesota) for helpful discussions, assistance with primer design and statistical analysis, and Robin Stocks (Department of Laboratory Medicine and Pathology, University of Alberta) for assistance with immunostaining.

Abbreviations

BMP	bone morphogenetic protein
BRORIN	brain-specific chordin-like
CHRD	chordin
CHRD-like 1	chordin-like 1
CHRD-like 2	chordin-like 2
CSF	cerebrospinal fluid
HPE	holoprosencephaly
Msx1	homeobox, msh-like 1
Msx2	homeobox, msh-like 2
NOG	noggin
TGFβ	transforming growth factor beta
TWSG1	twisted gastrulation
WT	wild type

References

Anderson RM, Lawrence AR, Stottmann RW, Bachiller D, Klingensmith J. Chordin and noggin promote organizing centers of forebrain development in the mouse. Development. 2002; 129:4975–4987. [PubMed: 12397106]

Balemans W, Van Hul W. Extracellular regulation of BMP signaling in vertebrates: a cocktail of modulators. Dev Biol. 2002; 250:231–250. [PubMed: 12376100]

Berdal A, Molla M, Hotton D, Aioub M, Lezot F, Nefussi JR, Goubin G. Differential impact of MSX1 and MSX2 homeogenes on mouse maxillofacial skeleton. Cells Tissues Organs. 2009; 189:126–132. [PubMed: 18769023]

Bonaguidi MA, Peng CY, McGuire T, Falciglia G, Gobeske KT, Czeisler C, Kessler JA. Noggin expands neural stem cells in the adult hippocampus. J Neurosci. 2008; 28:9194–9204. [PubMed: 18784300]

Brodbelt A, Stoodley M. CSF pathways: a review. Br J Neurosurg. 2007; 21:510–520. [PubMed: 17922324]

Buddensiek J, Dressel A, Kowalski M, Storch A, Sabolek M. Adult cerebrospinal fluid inhibits neurogenesis but facilitates gliogenesis from fetal rat neural stem cells. J Neurosci Res. 2009; 87:3054–3066. [PubMed: 19530161]

Chae TH, Kim S, Marz KE, Hanson PI, Walsh CA. The hyh mutation uncovers roles for alpha Snap in apical protein localization and control of neural cell fate. Nat Genet. 2004; 36:264–270. [PubMed: 14758363]

Crews L, Wyss-Coray T, Masliah E. Insights into the pathogenesis of hydrocephalus from transgenic and experimental animal models. Brain Pathol. 2004; 14:312–316. [PubMed: 15446587]

Dattatreyamurty B, Roux E, Horbinski C, Kaplan PL, Robak LA, Beck HN, Lein P, Higgins D, Chandrasekaran V. Cerebrospinal fluid contains biologically active bone morphogenetic protein-7. Exp Neurol. 2001; 172:273–281. [PubMed: 11716552]

Davy BE, Robinson ML. Congenital hydrocephalus in hy3 mice is caused by a frameshift mutation in Hydin, a large novel gene. Hum Mol Genet. 2003; 12:1163–1170. [PubMed: 12719380]

Delaune E, Lemaire P, Kodjabachian L. Neural induction in Xenopus requires early FGF signalling in addition to BMP inhibition. Development. 2005; 132:299–310. [PubMed: 15590738]

Di-Gregorio A, Sancho M, Stuckey DW, Crompton LA, Godwin J, Mishina Y, Rodriguez TA. BMP signalling inhibits premature neural differentiation in the mouse embryo. Development. 2007; 134:3359–3369. [PubMed: 17699604]

Dietrich P, Shanmugasundaram R, Shuyu E, Dragatsis I. Congenital hydrocephalus associated with abnormal subcommissural organ in mice lacking huntingtin in Wnt1 cell lineages. Hum Mol Genet. 2009; 18:142–150. [PubMed: 18838463]

Ebendal T, Bengtsson H, Soderstrom S. Bone morphogenetic proteins and their receptors: potential functions in the brain. J Neurosci Res. 1998; 51:139–146. [PubMed: 9469567]

Fan X, Xu H, Cai W, Yang Z, Zhang J. Spatial and temporal patterns of expression of Noggin and BMP4 in embryonic and postnatal rat hippocampus. Brain Res Dev Brain Res. 2003; 146:51–58.

Galbreath E, Kim SJ, Park K, Brenner M, Messing A. Overexpression of TGF-beta 1 in the central nervous system of transgenic mice results in hydrocephalus. J Neuropathol Exp Neurol. 1995; 54:339–349. [PubMed: 7745433]

Graf D, Timmons PM, Hitchins M, Episkopou V, Moore G, Ito T, Fujiyama A, Fisher AG, Merkenschlager M. Evolutionary conservation, developmental expression, and genomic mapping of mammalian Twisted gastrulation. Mamm Genome. 2001; 12:554–560. [PubMed: 11420619]

Johanson CE, Palm DE, Primiano MJ, McMillan PN, Chan P, Knuckey NW, Stopa EG. Choroid plexus recovery after transient forebrain ischemia: role of growth factors and other repair mechanisms. Cell Mol Neurobiol. 2000; 20:197–216. [PubMed: 10696510]

Krizhanovsky V, Ben-Arie N. A novel role for the choroid plexus in BMP-mediated inhibition of differentiation of cerebellar neural progenitors. Mech Dev. 2006; 123:67–75. [PubMed: 16325379]

Landrieu P, Ninane J, Ferriere G, Lyon G. Aqueductal stenosis in X-linked hydrocephalus: a secondary phenomenon? Dev Med Child Neurol. 1979; 21:637–642. [PubMed: 574474]

Larman BW, Karolak MJ, Adams DC, Oxburgh L. Chordin-like 1 and twisted gastrulation 1 regulate BMP signaling following kidney injury. J Am Soc Nephrol. 2009; 20:1020–1031. [PubMed: 19357253]

Larrain J, Oelgeschlager M, Ketpura NI, Reversade B, Zakin L, De Robertis EM. Proteolytic cleavage of Chordin as a switch for the dual activities of Twisted gastrulation in BMP signaling. Development. 2001; 128:4439–4447. [PubMed: 11714670]

Lein ES, Hawrylycz MJ, Ao N, Ayres M, Bensinger A, Bernard A, Boe AF, Boguski MS, Brockway KS, Byrnes EJ, Chen L, Chen TM, Chin MC, Chong J, Crook BE, Czaplinska A, Dang CN, Datta S, Dee NR, Desaki AL, Desta T, Diep E, Dolbeare TA, Donelan MJ, Dong HW, Dougherty JG, Duncan BJ, Ebbert AJ, Eichele G, Estin LK, Faber C, Facer BA, Fields R, Fischer SR, Fliss TP, Frensley C, Gates SN, Glattfelder KJ, Halverson KR, Hart MR, Hohmann JG, Howell MP, Jeung DP, Johnson RA, Karr PT, Kawal R, Kidney JM, Knapik RH, Kuan CL, Lake JH, Laramee AR, Larsen KD, Lau C, Lemon TA, Liang AJ, Liu Y, Luong LT, Michaels J, Morgan JJ, Morgan RJ, Mortrud MT, Mosqueda NF, Ng LL, Ng R, Orta GJ, Overly CC, Pak TH, Parry SE, Pathak SD, Pearson OC, Puchalski RB, Riley ZL, Rockett HR, Rowland SA, Royall JJ, Ruiz MJ, Sarno NR, Schaffnit K, Shapovalova NV, Sivisay T, Slaughterbeck CR, Smith SC, Smith KA, Smith BI, Sodt

AJ, Stewart NN, Stumpf KR, Sunkin SM, Sutram M, Tam A, Teemer CD, Thaller C, Thompson CL, Varnam LR, Visel A, Whitlock RM, Wohnoutka PE, Wolkey CK, Wong VY, Wood M, Yaylaoglu MB, Young RC, Youngstrom BL, Yuan XF, Zhang B, Zwingman TA, Jones AR. Genome-wide atlas of gene expression in the adult mouse brain. Nature. 2007; 445:168–176. [PubMed: 17151600]

Lim DA, Tramontin AD, Trevejo JM, Herrera DG, Garcia-Verdugo JM, Alvarez-Buylla A. Noggin antagonizes BMP signaling to create a niche for adult neurogenesis. Neuron. 2000; 28:713–726. [PubMed: 11163261]

Lindeman GJ, Dagnino L, Gaubatz S, Xu Y, Bronson RT, Warren HB, Livingston DM. A specific, nonproliferative role for E2F-5 in choroid plexus function revealed by gene targeting. Genes Dev. 1998; 12:1092–1098. [PubMed: 9553039]

Liu A, Niswander LA. Bone morphogenetic protein signalling and vertebrate nervous system development. Nat Rev Neurosci. 2005; 6:945–954. [PubMed: 16340955]

MacKenzie B, Wolff R, Lowe N, Billington CJ Jr, Peterson A, Schmidt B, Graf D, Mina M, Gopalakrishnan R, Petryk A. Twisted gastrulation limits apoptosis in the distal region of the mandibular arch in mice. Dev Biol. 2009; 328:13–23. [PubMed: 19389368]

Makiyama Y, Shoji S, Mizusawa H. Hydrocephalus in the Otx2+/− mutant mouse. Exp Neurol. 1997; 148:215–221. [PubMed: 9398463]

Marshall OJ. PerlPrimer: cross-platform, graphical primer design for standard, bisulphite and real-time PCR. Bioinformatics. 2004; 20:2471–2472. [PubMed: 15073005]

Martinez G, Carnazza ML, Di Giacomo C, Sorrenti V, Vanella A. Expression of bone morphogenetic protein-6 and transforming growth factor-beta1 in the rat brain after a mild and reversible ischemic damage. Brain Res. 2001; 894:1–11. [PubMed: 11245809]

Massague J, Seoane J, Wotton D. Smad transcription factors. Genes Dev. 2005; 19:2783–2810. [PubMed: 16322555]

Matsuo I, Kuratani S, Kimura C, Takeda N, Aizawa S. Mouse Otx2 functions in the formation and patterning of rostral head. Genes Dev. 1995; 9:2646–2658. [PubMed: 7590242]

Mehler MF, Mabie PC, Zhang D, Kessler JA. Bone morphogenetic proteins in the nervous system. Trends Neurosci. 1997; 20:309–317. [PubMed: 9223224]

Melnick M, Petryk A, Abichaker G, Witcher D, Person AD, Jaskoll T. Embryonic salivary gland dysmorphogenesis in Twisted gastrulation deficient mice. Arch Oral Biol. 2006; 51:433–438. [PubMed: 16289463]

Nosaka T, Morita S, Kitamura H, Nakajima H, Shibata F, Morikawa Y, Kataoka Y, Ebihara Y, Kawashima T, Itoh T, Ozaki K, Senba E, Tsuji K, Makishima F, Yoshida N, Kitamura T. Mammalian twisted gastrulation is essential for skeleto-lymphogenesis. Mol Cell Biol. 2003; 23:2969–2980. [PubMed: 12665593]

Ovchinnikov DA, Selever J, Wang Y, Chen YT, Mishina Y, Martin JF, Behringer RR. BMP receptor type IA in limb bud mesenchyme regulates distal outgrowth and patterning. Dev Biol. 2006; 295:103–115. [PubMed: 16630606]

Park C, Lavine K, Mishina Y, Deng CX, Ornitz DM, Choi K. Bone morphogenetic protein receptor 1A signaling is dispensable for hematopoietic development but essential for vessel and atrioventricular endocardial cushion formation. Development. 2006; 133:3473–3484. [PubMed: 16887829]

Petryk A, Anderson RM, Jarcho MP, Leaf I, Carlson CS, Klingensmith J, Shawlot W, O'Connor MB. The mammalian twisted gastrulation gene functions in foregut and craniofacial development. Dev Biol. 2004; 267:374–386. [PubMed: 15013800]

Petryk A, Shimmi O, Jia X, Carlson AE, Tervonen L, Jarcho MP, O'Connor MB, Gopalakrishnan R. Twisted gastrulation and chordin inhibit differentiation and mineralization in MC3T3-E1 osteoblast-like cells. Bone. 2005; 36:617–626. [PubMed: 15780974]

Ramos C, Fernandez-Llebrez P, Bach A, Robert B, Soriano E. Msx1 disruption leads to diencephalon defects and hydrocephalus. Dev Dyn. 2004; 230:446–460. [PubMed: 15188430]

Redzic ZB, Preston JE, Duncan JA, Chodobski A, Szmydynger-Chodobska J. The choroid plexus-cerebrospinal fluid system: from development to aging. Curr Top Dev Biol. 2005; 71:1–52. [PubMed: 16344101]

Rickert CH, Paulus W. Tumors of the choroid plexus. Microsc Res Tech. 2001; 52:104–111. [PubMed: 11135453]

Rosenthal A, Jouet M, Kenwrick S. Aberrant splicing of neural cell adhesion molecule L1 mRNA in a family with X-linked hydrocephalus. Nat Genet. 1992; 2:107–112. [PubMed: 1303258]

Ross JJ, Shimmi O, Vilmos P, Petryk A, Kim H, Gaudenz K, Hermanson S, Ekker SC, O'Connor MB, Marsh JL. Twisted gastrulation is a conserved extracellular BMP antagonist. Nature. 2001; 410:479–483. [PubMed: 11260716]

Schiffer C, Tariverdian G, Schiesser M, Thomas MC, Sergi C. Agnathia-otocephaly complex: report of three cases with involvement of two different Carnegie stages. Am J Med Genet. 2002; 112:203–208. [PubMed: 12244557]

Scott IC, Steiglitz BM, Clark TG, Pappano WN, Greenspan DS. Spatiotemporal expression patterns of mammalian chordin during postgastrulation embryogenesis and in postnatal brain. Dev Dyn. 2000; 217:449–456. [PubMed: 10767089]

Sieber C, Kopf J, Hiepen C, Knaus P. Recent advances in BMP receptor signaling. Cytokine Growth Factor Rev. 2009; 20:343–355. [PubMed: 19897402]

Soderstrom S, Bengtsson H, Ebendal T. Expression of serine/threonine kinase receptors including the bone morphogenetic factor type II receptor in the developing and adult rat brain. Cell Tissue Res. 1996; 286:269–279. [PubMed: 8854897]

Soderstrom S, Ebendal T. Localized expression of BMP and GDF mRNA in the rodent brain. J Neurosci Res. 1999; 56:482–492. [PubMed: 10369215]

Strazielle N, Ghersi-Egea JF. Choroid plexus in the central nervous system: biology and physiopathology. J Neuropathol Exp Neurol. 2000; 59:561–574. [PubMed: 10901227]

Sun M, Thomas MJ, Herder R, Bofenkamp ML, Selleck SB, O'Connor MB. Presynaptic contributions of chordin to hippocampal plasticity and spatial learning. J Neurosci. 2007; 27:7740–7750. [PubMed: 17634368]

Tada T, Zhan H, Tanaka Y, Hongo K, Matsumoto K, Nakamura T. Intraventricular administration of hepatocyte growth factor treats mouse communicating hydrocephalus induced by transforming growth factor beta1. Neurobiol Dis. 2006; 21:576–586. [PubMed: 16352434]

Tang J, Song M, Wang Y, Fan X, Xu H, Bai Y. Noggin and BMP4 co-modulate adult hippocampal neurogenesis in the APP(swe)/PS1(DeltaE9) transgenic mouse model of Alzheimer's disease. Biochem Biophys Res Commun. 2009; 385:341–345. [PubMed: 19463786]

Willems PJ, Brouwer OF, Dijkstra I, Wilmink J. X-linked hydrocephalus. Am J Med Genet. 1987; 27:921–928. [PubMed: 3425602]

Wills A, Harland RM, Khokha MK. Twisted gastrulation is required for forebrain specification and cooperates with Chordin to inhibit BMP signaling during X. tropicalis gastrulation. Dev Biol. 2006; 289:166–178. [PubMed: 16321373]

Wyss-Coray T, Feng L, Masliah E, Ruppe MD, Lee HS, Toggas SM, Rockenstein EM, Mucke L. Increased central nervous system production of extracellular matrix components and development of hydrocephalus in transgenic mice overexpressing transforming growth factor-beta 1. Am J Pathol. 1995; 147:53–67. [PubMed: 7604885]

Ybot-Gonzalez P, Gaston-Massuet C, Girdler G, Klingensmith J, Arkell R, Greene ND, Copp AJ. Neural plate morphogenesis during mouse neurulation is regulated by antagonism of Bmp signalling. Development. 2007; 134:3203–3211. [PubMed: 17693602]

Zakin L, De Robertis EM. Inactivation of mouse Twisted gastrulation reveals its role in promoting Bmp4 activity during forebrain development. Development. 2004; 131:413–424. [PubMed: 14681194]

Zakin L, Reversade B, Kuroda H, Lyons KM, De Robertis EM. Sirenomelia in Bmp7 and Tsg compound mutant mice: requirement for Bmp signaling in the development of ventral posterior mesoderm. Development. 2005; 132:2489–2499. [PubMed: 15843411]

Zhang J, Williams MA, Rigamonti D. Genetics of human hydrocephalus. J Neurol. 2006a; 253:1255–1266. [PubMed: 16773266]

Zhang W, Yi MJ, Chen X, Cole F, Krauss RS, Kang JS. Cortical thinning and hydrocephalus in mice lacking the immunoglobulin superfamily member CDO. Mol Cell Biol. 2006b; 26:3764–3772. [PubMed: 16648472]

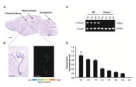

Figure 1. Expression pattern of *Twsg1* in a mouse adult brain

(A) *In situ* hybridization image from Allen Brain Atlas; sagittal section, 55 days old male. *Twsg1* is expressed in the choroid plexus, hippocampus, and cerebellum. (B) Close-up view of the choroid plexus with digital analysis of signal intensity. (C) RT-PCR data showing expression of *Twsg1* from different brain regions of WT mice, and absence of the transcript in $Twsg1^{-/-}$ mice. (D) Q-PCR data showing the highest level of *Twsg1* expression in the choroid plexus compared to other brain regions; no signal is detected from $Twsg1^{-/-}$ hippocampus (KO). BS, brain stem; CP, choroid plexus; CR, cerebellum; CX, cerebral cortex; HP, hippocampus; OB, olfactory bulb; TH, thalamus;. Beta-actin is the reference gene for the reactions. Scale bars: 824 μm in A and 314 μm in B.

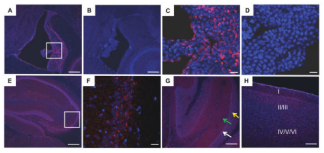

Figure 2. Immunolocalization of TWSG1 in adult mouse brain

(A) TWSG1 is detected at highest level in choroid plexus. (B) Negative control (no primary antibody). (C) Higher magnification of the region in A (box) showing patch-like staining of TWSG1 on cell surface and in the extracellular matrix in the choroid plexus. (D) Negative control. (E) Hippocampus. (F) Higher magnification of the region in E (box); CA3 region of hippocampus shows patch-like TWSG1 staining. (G) Purkinje cell layer (white arrow) shows high TWSG1 expression in cerebellum. Weak immunoreactivity is present in the granular layer (green arrow), but not molecular layer (yellow arrow). (H) Cortical neurons show weak immunoreactivity for TWSG1, particularly in layer II/III. Scale bars: 200 μm in A, B, E, G, H and 20 μm in C, D, F.

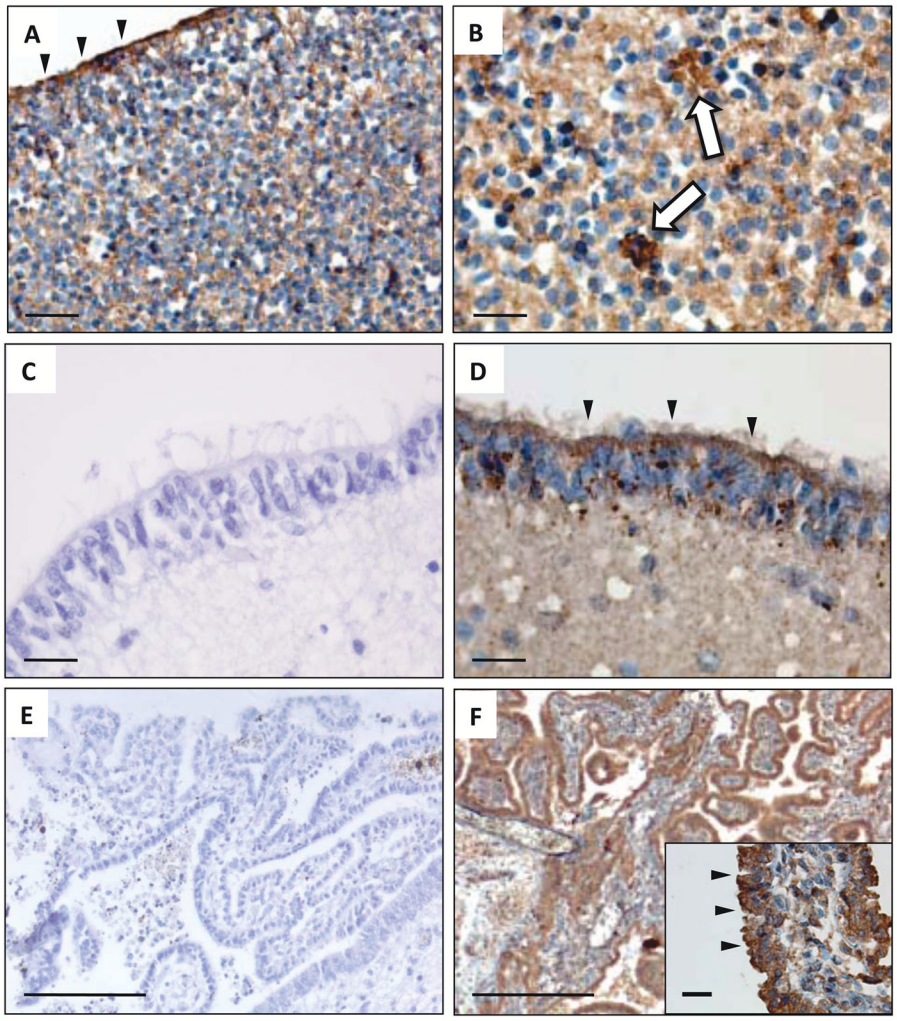

Figure 3. Immunolocalization of TWSG1 in human fetal brain at mid-gestation

(A) Cerebral cortex. Arrowheads point to the molecular layer. (B) Cerebral cortex. Intense staining in the perikarya of neurons with rosette pattern formation (Fig. 6B, arrows). (C) Control staining of fetal brain without primary antibody (negative control); 630x magnification. (D) Ventricular epithelium of the 4th ventricle showed moderate immunoreactivity. Arrowheads point to the ependymal epithelium. (E) Negative control; 100x magnification. (F) Choroid plexus. The strongest expression was observed in the choroid plexus. Inset at 630x magnification, all papillary projections of the choroid plexus show an intense signal of the lining epithelium, whereas no signal is seen in the fibrovascular core of the papillary projections. Scale bars: 20 μm in A–D and inset and 200 μm in E, F.

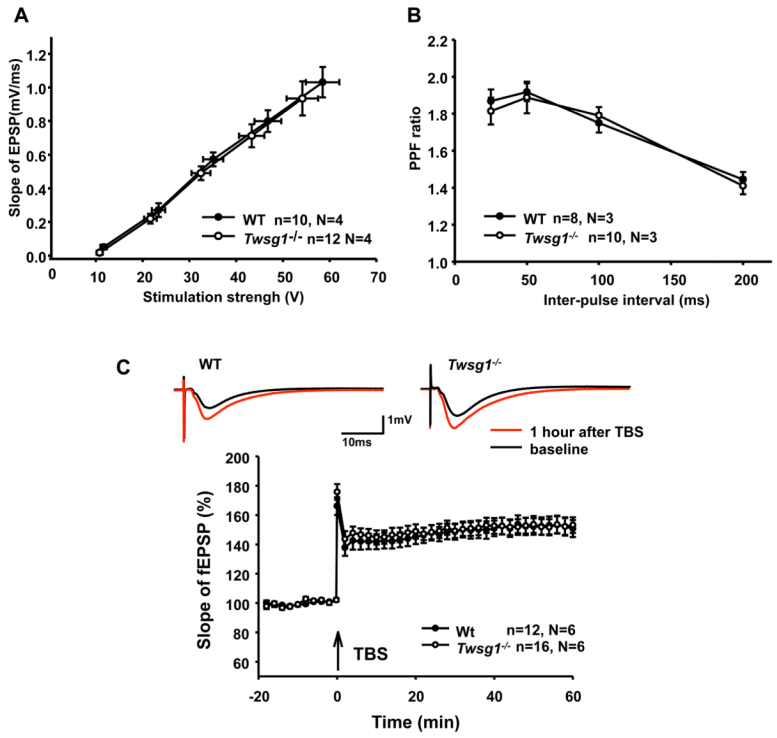

Figure 4. Electrophysiological evaluation of synaptic plasticity in the hippocampus

(A) Normal input-output curve in hippocampal synaptic transmission in *Twsg1*$^{-/-}$ mice. Relationship between the slope of fEPSP (field excitatory postsynaptic potential) and stimulation strength for *Twsg1*$^{-/-}$ and WT mice. Data are expressed as mean ± SEM. (B) Normal Paired-pulse facilitation (PPF) in *Twsg1*$^{-/-}$ hippocampal slices. PPF was measured as the ratio between the slopes of fEPSPs evoked by the second and first pulses and plotted for several inter-pulse intervals (ISI). Field EPSPs were evoked with a stimulus that evoked 30% of the maximal fEPSP. Values represent mean ± SEM. (C) TBS protocol induced a similar level of LTP in *Twsg1*$^{-/-}$ and WT slices. Mean amplitudes of fEPSPs recorded 0–20 min before induction of LTP were set as a baseline. Above the summary plot are shown an average baseline sweep and a sweep 1 hour after induction.

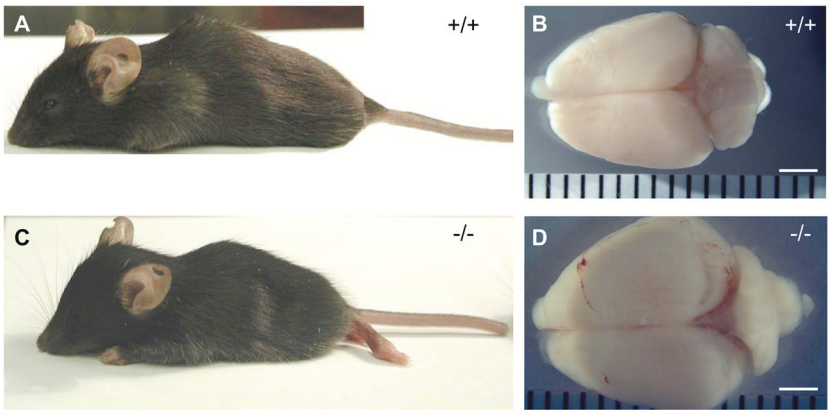

Figure 5. Severe hydrocephalus in TWSG1-deficient mice

(A) WT male mouse at 1 month of age. (B) A gross view of a WT brain. (C) *Twsg1*$^{-/-}$ mice have smaller body size but larger brain volume (D) in comparison with WT littermates in C57BL/6 background. Knockout mice show enlarged head with dome-shape skull and partly closed eyes. Scale bars: 2 mm in B, D.

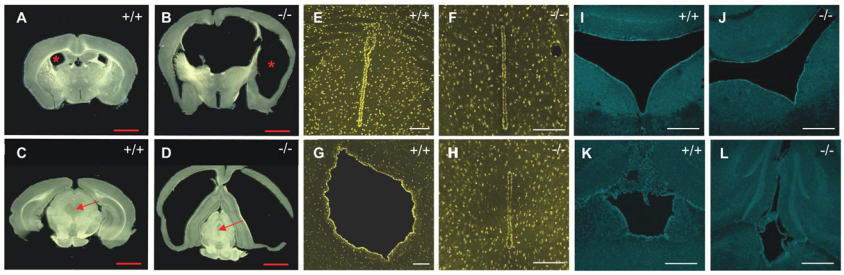

Figure 6. Ventricular system in *Twsg1*$^{-/-}$ mice and controls

(A) Coronal section through WT brain. (B) Coronal section through a *Twsg1*$^{-/-}$ brain with hydrocephalus showing enlarged lateral ventricles and third ventricle; the asterisk indicates the lateral ventricle. Also the cortex is atrophic and much thinner than control. (C) WT brain; arrow points to the periaqueductal grey matter. (D) Compressed hippocampi and aqueduct. (E–H) Serial sections through the aqueduct; DAPI staining with pseudocolor. (G) WT aqueduct; the largest opening is at midbrain interaural -1mm level. (H) Closed aqueduct in a mutant. (I, J) Normal fourth ventricle and (K,L) normal choroid plexus tissue in the dorsal part of third ventricle. There was no evidence of papilloma in any of the ventricles. Scale bars: 2 mm in A–D, 100 μm in E–H, 200 μm in I–L.

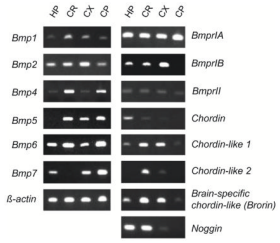

Figure 7. Expression of BMP ligands, their receptors, and BMP-binding proteins in a mouse brain at 1 month of age by RT-PCR

The brain regions tested included hippocampus (HP), cerebellum (CR), cerebral cortex (CX), and choroid plexus (CP). All *Bmps* tested, *BmprIA*, *BmprII*, *Chrd-like 1* and *Brorin* were expressed in the choroid plexus, but not *Chrd*, *Chrd-like 2*, or *Nog*.

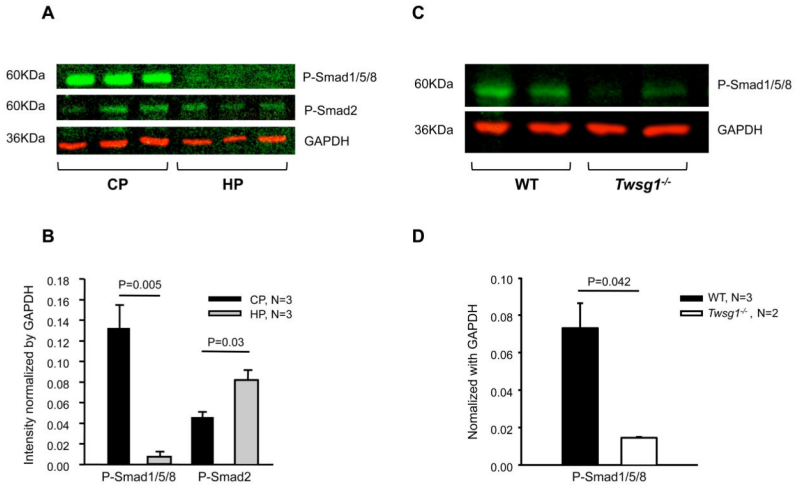

Figure 8. Comparison between the levels of BMP and TGFβ signaling in the choroid plexus and the hippocampus by western blotting

(A) Representative image shows the western blot double-staining with anti-P-Smads and GAPDH antibodies. (B) BMP signaling is more active in the choroid plexus than in the hippocampus in WT mice. Conversely, P-Smad2 signaling is significantly lower in the choroid plexus than in the hippocampus. (C) Representative gel image shows reduced P-Smad1/5/8 signal in *Twsg1*$^{-/-}$ choroid plexus with GAPDH as a control. (D) The graph shows significantly lower P-Smad1/5/8 level in *Twsg1*$^{-/-}$choroid plexus compared to WT.

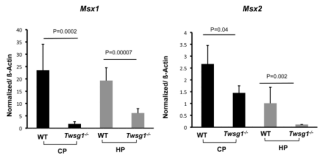

Figure 9. Downstream targets of BMP signaling pathway are suppressed in *Twsg1*$^{-/-}$ choroid plexus and hippocampus

Both *Msx1* and *Msx2*, two major BMP regulated genes in neural tissues, are reduced in *Twsg1*$^{-/-}$ choroid plexus and hippocampus. The samples were obtained from 3 wild type and 3 *Twsg1*$^{-/-}$ mice.

Table 1

PCR primer sequences

Gene	Forward [5′–3′]	Reverse [5′–3′]
Bmp1	TTTCAAAGAGGTGGATGAGTG	AAGAAGTCAAATTGCAGGGAG
Bmp2	TGGAAGTGGCCCATTTAGAG	TGACGCTTTTCTCGTTTGTG
Bmp4	TCCATCACGAAGAACATCTG	TAGTCTGGTGTCCAGTAGTC
Bmp5	CTGGCTTGTCTTTGATATCAC	TATTATAATCTCCAGCACTGGG
Bmp6	GCTGGAATTTGACATCACAG	CCGTTGTAGTCTGAAGAACC
Bmp7	TCAACCTAGTGGAACATGAC	GATAGACTGTGATCTGGAAGG
BmprIa	CTTCTCCAGCTGCTTTTGCT	ATAGCGGCCTTTACCAACCT
BmprIb	ATGTGTTTCTGGAGGTATAGTG	GCTCTGTCCACAAGTATCTG
BmprII	TGGCAGTGAGGTCACTCAAG	TTGCGTTCATTCTGCATAGC
Chordin	CAGTGACACAGAAGATTCCT	TTTGAAGGACATCACAGCTC
Chordin-like 1	CAAGTCATGCGAATACAATGG	AGGTAAGAATGTCTTGCTTCTC
Chordin-like 2	CAATATCCCTGCAGTCAACC	GTGGTAGATTCCTTTCACCAG
Brorin	AGACCTACCAGACTTTGGAG	CCTCTTCATAAGTGCAGTGAC
Noggin	AAGAAGCTGAGGAGGAAGTT	GACTTGGATGGCTTACACAC
Twsg1	CTGAACTGGAACATCGTCTC	GCAGTCATCAAAGTAAACCAC
s-actin	GTGTGATGGTGGGAATGGGT	GGTCTCAAACATGATCTGGGTC

Table 2

Survival rate of *Twsg1*$^{-/-}$ mice born to *Twsg1*$^{+/-}$ dams in C57BL/6 background

Frequency	Outcome
44%	Survive beyond 3 weeks of life, smaller size, short/kinky tails, normal fertility; 4.3% develop severe hydrocephalus.
45%	Die within the first 24 hours of life due to craniofacial defects (holoprosencephaly, midline facial defects, agnathia, cyclopia, proboscis, anterior truncation)
11%	Die at birth or within the first 48 hours to 2 weeks of life without external craniofacial defects.